The Response of Surface-Level Atmospheric Electrical Parameters in Israel to Severe Space Weather Events

Roy Yaniv , Yoav Yosef Yair * , Colin Gregory Price , Yuval Reuveni

Posted Date: 4 October 2023

doi: 10.20944/preprints202310.0209.v1

Keywords: space weather; global electric circuit; fair weather; electric field; current density; solar proton events; coronal mass ejection

Article

The Response of Surface-Level Atmospheric Electrical Parameters in Israel to Severe Space Weather Events

Roy Yaniv [1,2], Yoav Yair [2,*], Colin Price [3] and Yuval Reuveni [4,5]

[1] Institute of Earth Sciences, The Hebrew University of Jerusalem, Israel
[2] School of Sustainability, Reichman University, Herzliya, Israel
[3] School of Geosciences, Tel Aviv university, Israel
[4] East R&D center, Ariel, Israel
[5] Department of Physics, Ariel University, Ariel, Israel
* Correspondence: yoav.yair@runi.ac.il; Tel.: +972-99527953; Fax: +972-525415091

Abstract: We report on ground-based measurements of the atmospheric electric field (Ez= -Potential Gradient (PG)) and current density (Jz) that were conducted at two locations in Israel. One is the Emilio Segre cosmic ray station located on Mt. Hermon (34.45 N, 2020 m AMSL) located in northern Israel near the Syrian-Lebanon border and at the other at the Wise astronomical observatory in the Negev desert highland plateau of southern Israel (31.18 N, 870 m AMSL). We searched for possible effects of strong, short-term solar events on the potential gradient and the vertical current density, as disruption to the Global Electric Circuit are often observed following strong solar events. The first case study (St. Patrick Day, 17 March 2015) was classified as the strongest event of 2015. The second case study (8 Sep 2017) was categorized as the strongest event of 2017 and one of the twenty strongest events on record to date. The results show that the electrical parameters measured at ground level at both stations were not affected during the two massive proton events and the ensuing geomagnetic storms. The magnetospheric shielding in lower latitudes is strong enough to shield against flux of energetic particles from solar events, obscuring any impact that may be noticeable above the local daily variations induced by local meteorological conditions (aerosol concentrations, clouds, high humidity, and wind speed) which were investigated as well.

Keywords: space weather; global electric circuit; fair weather; electric field; current density; solar proton events; coronal mass ejection

1. Introduction

Earth's atmosphere undergoes continuous interactions with various types of energetic particles coming from space and from the sun. Solar energetic particles (SEP) contain 100s KeV electrons and tens MeV protons which deposit their energy in the atmosphere, altering the chemistry and the ionization in the upper atmosphere (Rycroft et al., 2000). Coronal Mass Ejections (CMEs) and solar flares feature thermal particles moving with a magnetized plasma that are expelled from the sun with velocities of hundreds to thousands km s^{-1} (Rycroft et al., 2000). Upon arrival at Earth, CMEs and solar flares induce pressure on the magnetosphere, thus generating enhanced and disruptive geomagnetic storms. Geomagnetic storms occur when the solar magnetic shock front reconnects with Earth's geomagnetic field, generating ring currents (Rycroft et al., 2000; Hudson, 2011; Rycroft et al., 2012). The rapid decrease in the intensity of Galactic Cosmic Rays (GCR) radiation reaching earth following a solar event is caused by the magnetic field of the solar wind sweeping some of the GCR flux away from Earth in what is known as Forbush decrease (Zhao and Zhang, 2016; Mironova et al 2015). The Forbush decrease can be detected by ground muon detectors for the duration of the impact which can be several hours long with a gradual recovery of the cosmic ray flux in the next hours to days (Usoskin et al., 2008). A typical Forbush decrease has a magnitude of 4-5% of the normal value as measured at ground level by neutron monitors. The rate of occurrence of the phenomena is influenced by the 11 years cycle of the sun, and is much more frequent during the years of solar

maximum. The GCR ionization rate exhibits around 10% difference from solar maximum to solar minimum (Bazilevskaya et al., 2008; Mironova et al., 2015).

The Global Electric Circuit (GEC) is a conceptual scheme that refers to the electrical activity in the medium between two conducting plates – the lower ionosphere and the highly conducting Earth – which both serve as the top and bottom plates of a postulated "spherical capacitor". Together with the atmospheric dielectric medium between them, and the thunderstorms that act as generators, they define a closed circuit, in which a vertical current (Jz) flows to the ground in fair-weather regions (Rycroft et al., 2000; 2012; Haldoupis et al., 2017). Short term variations in the ionization rate at higher altitudes due to changes in the GCR flux, which can last from several hours to several days due to solar events, will affect the GEC by altering the conductivity and the columnar atmospheric resistance. Therefore, and in compliance with Ohm's law, we should expect changes in the vertical electric E-field (Ez) or the Potential gradient (PG = -Ez).

Ground measurements during times of solar events affecting the Earth at polar latitudes show a decrease in the potential gradient from fair weather values (~-130 V m^{-1} at sea level) to tenths and even zero V m^{-1} values. The decrease in the potential gradient in polar latitudes is a result of the increased conductivity, an effect of the enhanced ionization due to injection of charged particles, e.g. electrons, protons and ions, which are funneled to the polar latitudes by the Earth's magnetic field (Holzworth and Mozer, 1981; Holzworth et al., 1987; Tinsley, 1996; Rycroft et al., 2000; Nikiforova et al., 2005).

Contrary to the above, ground measurements conducted at high and mid latitudes at times of SEPs and CMEs show an increase of the potential gradient and of the conduction current (Jz). This was observed on the day of the impact and in subsequent days (Cobb, 1967; Reiter, 1969; Kasatkina et al., 2009). Mid-latitude measurements of PG and Jz conducted by the network of middle and high-latitude observatories in Europe (~45N-60N) following six events of Forbush decrease showed an immediate increase when the GCR ionization rate was at a minimum (Sheftel et al., 1994). Measurements of the PG at Swider, Poland (52.2 N geographic, 53.9N magnetic, geomagnetic rigidity cutoff ~3 GV) during 14 strong and moderate magnetic storms occurring in days defined as fair weather (based on meteorology) found an influence of the solar events on the PG which exceeded local fair weather variation by ~150 V m^{-1}. The PG amplitude changes were correlated with the times of Forbush decrease events (Kleimenova et al., 2009). Ground measurements of the potential gradient in Kamchatka, Russia (57° N geographic, 58.5°N magnetic) showed amplitudes of up to 300 V m^{-1} during a geomagnetic storm in 2010 (Smirnov, 2014). Qiu et. al. (2022) reported 15 cases of increased geomagnetic activity at mid latitudes which found variations that range between 100-600 V m^{-1} compared to fair weather values.

Airborne stratospheric measurements during a solar flare at high (50-70° N) and low (<50 N) latitudes found a short duration increase by a factor of 2 in the current density (Jz) at high latitudes but no effect in lower latitude (Holzworth, 1981; Holzworth et al., 1987). Simultaneous ground and airborne measurements were performed at Reading, UK (51.4°N geographic, 53.12°N magnetic, and geomagnetic rigidity cutoff 3.6 GV) during a solar flare. An X-ray burst followed by a solar proton event (SEP) resulted in observed changes in the PG and the Jz at ground level and an increase of the ionization in the troposphere (Nicoll and Harrison, 2014). Elhalel et al. (2014) investigated the short-term influence of solar disturbances on the fair-weather current (Jz) at the Wise Observatory, Israel, during three solar events – two CMEs and one SEP. The results showed an increase by one order of magnitude in the Jz variance, which were inconclusive since an impact of the local surface wind could not be ruled out (it should be noted that no PG measurement were available at that time). More recently, Tacza et al. (2018) measured the effect of solar events on the PG at a low latitude station in Argentina (31.798° S geographic, 21.95 S magnetic, geomagnetic rigidity cutoff 9.8 GV) and found a noticeably low impact of ~10-15 V m^{-1} variation from fair weather values.

2. Instrumentation and Observation Sites

In the present study, we rely upon the infrastructure that exists at two measuring sites, and we will review it here briefly. The instruments are located at two permanent sites operated by Tel-Aviv

Preprints (www.preprints.org) | NOT PEER-REVIEWED | Posted: 4 October 2023 doi:10.20944/preprints202310.0209.v1

University, through collaborative research with Ariel University and the Reichman University, Herzliya. The Wise observatory site in Mitzpe Ramon (30°35'N, 34°45'E, altitude 850 meter above sea level, geomagnetic 27° 6'N 112° 23'E, geomagnetic rigidity cutoff 10.3 GV), is located near the town Mitzpe Ramon (MR) is an arid plateau in the southern part of Israel (Negev desert). The second site is on Mount Hermon (33°18'N 35°47.2'E, altitude of ~2100 meter above sea level, geomagnetic 29° 36'N 113°° 56'E, geomagnetic rigidity cutoff 10.1 GV) which is the highest peak in Israel.

Fair weather ground measurements of the vertical electric field (Ez) are being conducted intermittently since June 2013 and April 2015 at Mitzpe Ramon (MR) and Mount Hermon, respectively. The diurnal fair-weather curves shown in Figure 1 were obtained on dates which are defined meteorologically as fair weather days. Fair weather in this context is defined as weather with clear skies or low amount of stratiform clouds (<3/8 cover), wind speed less than 8 m s^{-1} (or less than 30 km h^{-1}) and no precipitation or lightning activity (Harrison and Nicoll, 2018).Throughout the last decade, more capabilities were added to both stations, offering a solid, stable and clean environment for atmospheric and space weather studies. For observing the vertical component of the atmospheric electric field, we employ the CS110 field mill (Yaniv et al 2016, 2017). The vertical conduction current (Jz) in the atmosphere is monitored by the Geometrical Displacement and Conduction Current Sensor (GDACCS) developed at the Meteorology Department in the University of Reading, UK (Bennett and Harrison 2008, Yaniv et al., 2018). The mean diurnal PG values for the Wise Observatory are ~150 V/m during local night hours (5-6 UT), reflecting the minimum in the Carnegie Curve (Harrison, 2017) which is a manifestation of the low lightning activity in the Pacific Ocean. The mean value of the PG increases to ~200 V m^{-1} at local afternoon and early evening hours due to intense lightning activity in the Americas (21 UT), dominating the Carnegie curve. Yaniv and Yair (2022) and Yair and Yaniv (2023) found that low clouds, fog, high humidity and wind speed cause an increase of the measured ground PG at Mitzpe Ramon. The increase can be up to +30 V m^{-1} at times of low clouds and up to +150-300 V m^{-1} at times of fog conditions (high humidity and low wind speed) from fair weather values.

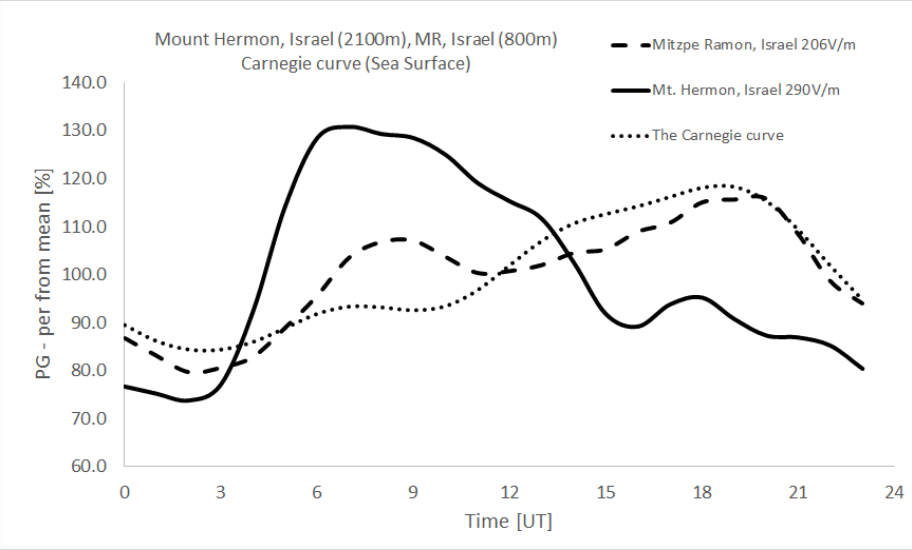

Figure 1. Diurnal fair weather curves from Mitzpe Ramon (Yaniv et al., 2016), Mount Hermon (Yaniv et al., 2017) and the Carnegie curve (Harrison 2013).

The mean PG values for Mount Hermon are around 200 V m^{-1} at night hours, the PG then increases to ~360 V m^{-1} during local late morning due to the "Austausch" effect and decreases again to ~260 V m^{-1} in the evening. The stations exhibit ±30 V m^{-1} and ±50 V m^{-1} variations respectively around the mean (Yaniv et al., 2016, 2017). The mean values of the conduction current density (Jz) measured at Mt. Hermon are in the range of 0.9-1.5 pA m^{-2} and are subjected to daily local variations due to aerosols, wind and local turbulence, as well as current flowing in the GEC due to global thunderstorm activity (Yaniv et al., 2018).

Preprints (www.preprints.org) | NOT PEER-REVIEWED | Posted: 4 October 2023 doi:10.20944/preprints202310.0209.v1

The Israel Cosmic Ray and Space Weather Station on Mt. Hermon (http://www.tau.ac.il/institutes/advanced/cosmic/icrc.htm) measures cosmic ray (CR) fluxes and the specific intensities of neutron multiplicities by using standard 6NM-64 boron trifluoride (BF_3) detectors with energy threshold of 10.6 GeV. The gamma radiation intensity at ground level is measured by using NaI (Tl) scintillation detectors (PM-11) tuned to the energy range of 50–3000 keV (Reuveni et al 2017). The observatory measures meteorological parameters such as pressure, relative humidity and temperature as well.

Solar activity, space weather and their impacts on Earth are monitored by the geostationary (35786km altitude) satellite GOES 13. The satellite measures the proton and electron fluxes. The data is plotted in near real-time and presented on NOAA website (https://satdat.ngdc.noaa.gov/) with an estimated Kp-index (global geomagnetic storm index) bar graphs. The list of events such as CMEs, Geomagnetic storms and Solar energetic particle events (SEP) detected by the satellites is available at NOAA website. The parameters (protons and electron flux) measured according to the GOES 13 satellite for the two events are shown in Figures (2a and 3a). We should note that the mean velocity of the solar particles can vary between 300-850 km s^{-1} (Rycroft et al. 2000, Kallenrode 2013) resulting in a time delay of 40-70 sec between the arrival of the particles to the satellite and when they interact with the Earth's atmosphere.

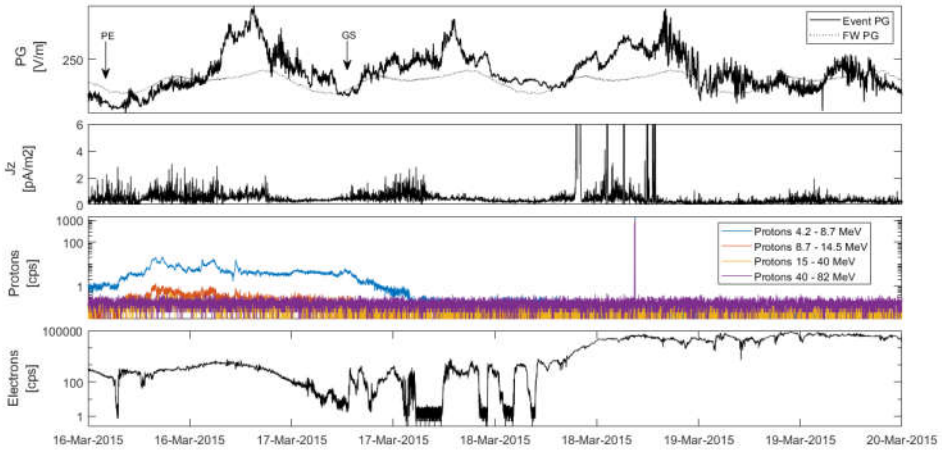

(**a**)

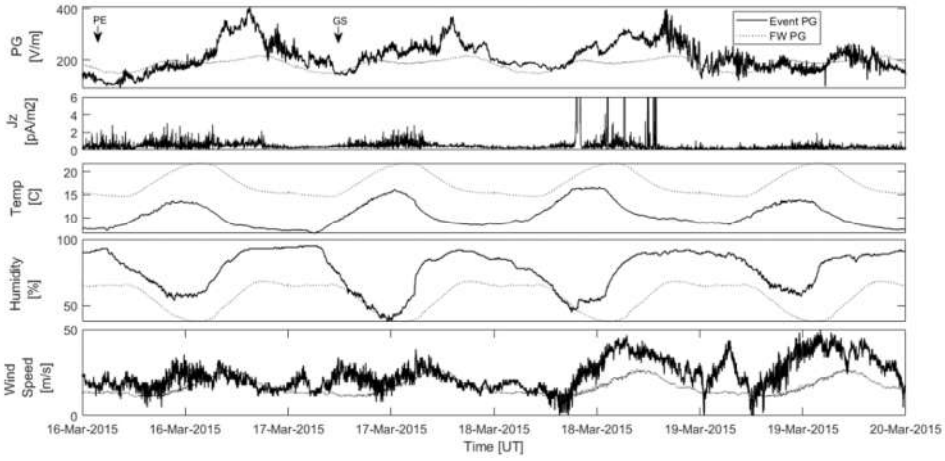

(**b**)

Preprints (www.preprints.org) | NOT PEER-REVIEWED | Posted: 4 October 2023 doi:10.20944/preprints202310.0209.v1

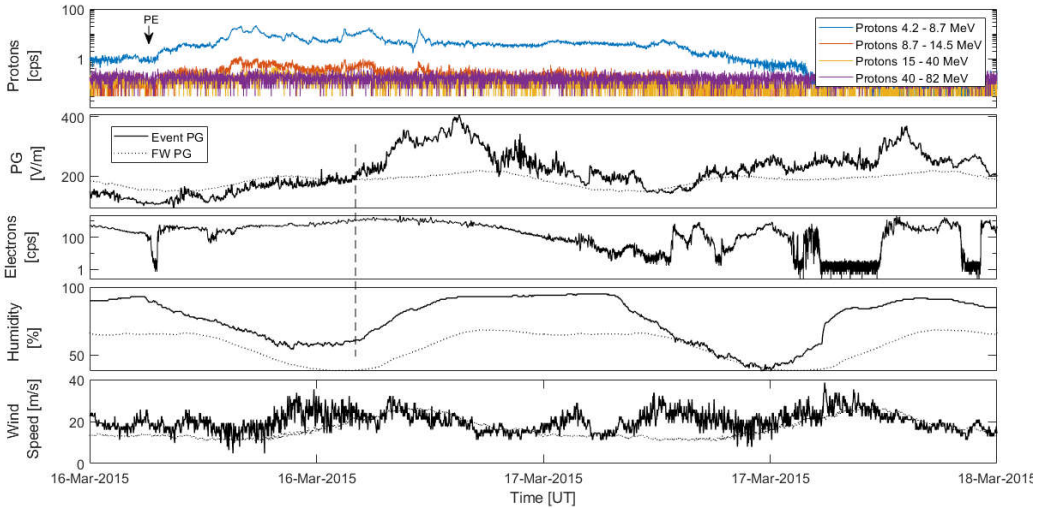

(c)

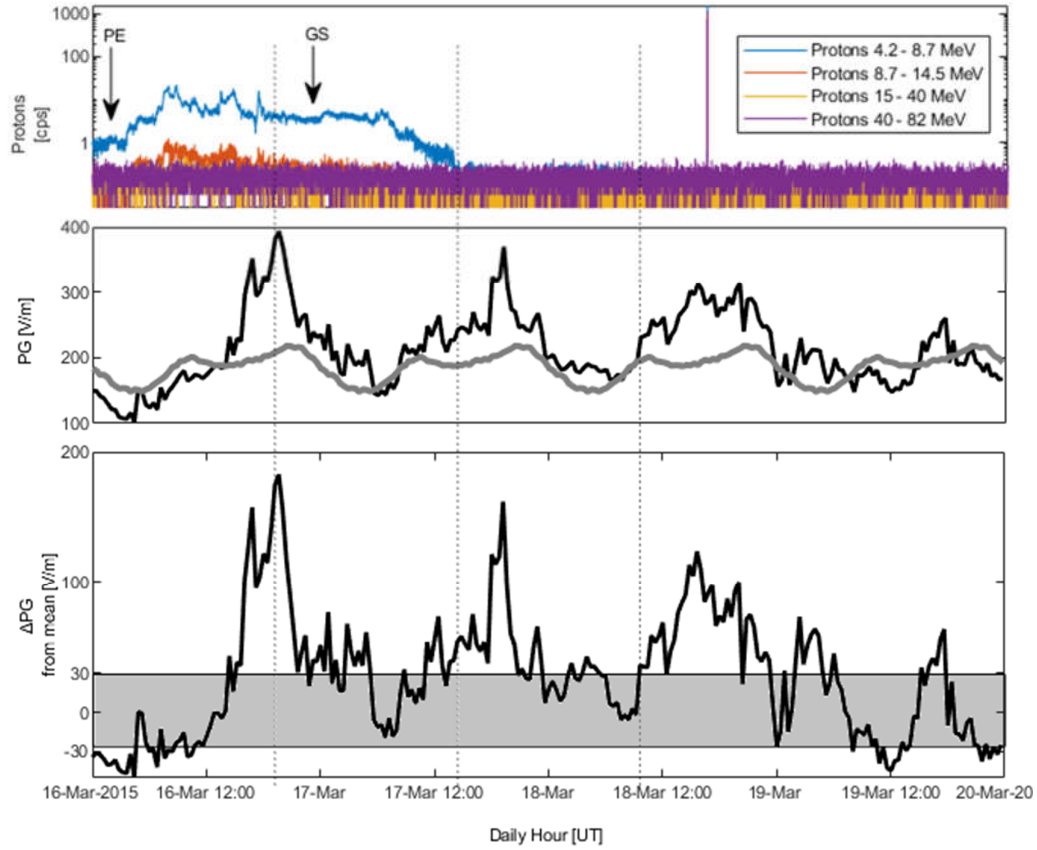

(d)

Preprints (www.preprints.org) | NOT PEER-REVIEWED | Posted: 4 October 2023 doi:10.20944/preprints202310.0209.v1

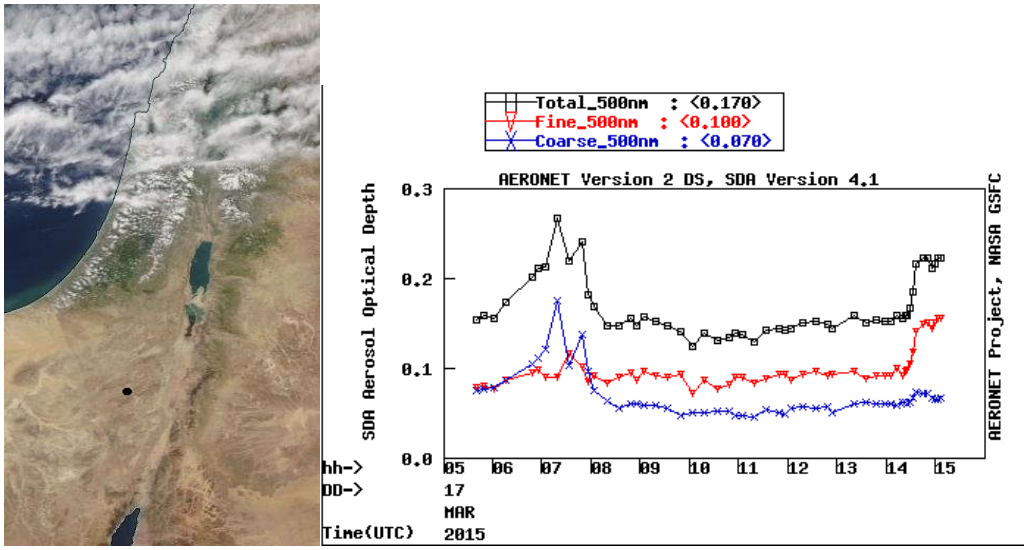

(**e**)

Figure 2. (**a**) 16-20 Mar 2015 Mitzpe Ramon station parameters: PG (top panel), Jz (Second panel) and the satellite environment measured by GOES 13 - proton and electron flux (bottom panels). (**b**) 16-20 Mar 2015 Mitzpe Ramon station parameters: PG (top panel), Conduction current Jz (Second panel) and meteorological parameters of temperature, humidity and wind speed (Bottom three panels). Dotted line are mean pattern of fair weather behavior. PE stands for the start of the proton event and GS is the start of the geomagnetic storm. (**c**) Mitzpe Ramon station zoom-in on the solar event 16 Mar 00:00 to 18 Mar 00:00 – the parameters are: Protons and electron flux, PG, Humidity and wind speed. Dashed line represents the time when humidity starts to increase. (**d**) ΔPG analysis. The solar proton flux with event time indication (top), PG values during the events and fair-weather mean behavior (middle) and ΔPG and standard deviation grayed area that show diurnal fair weather variations in the Ramon station (bottom). (**e**) Sat image of Israel from 17 Mar 2015 showing scattered low clouds at central and north regions and no clouds at all in the southern region. Black dot is the MR station (left). Daily average of fine and coarse particles AOD at 17 Mar 2015 (right).

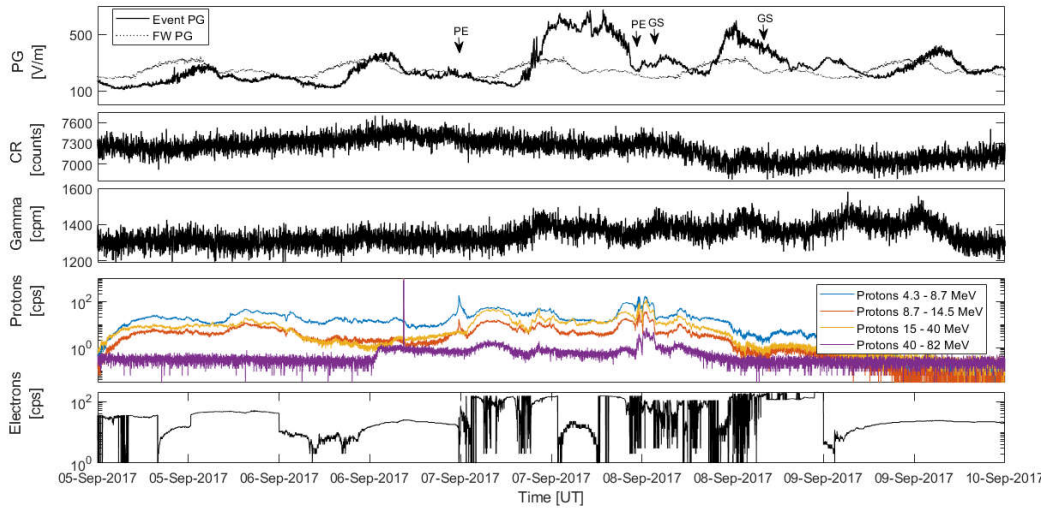

(**a**)

Preprints (www.preprints.org) | NOT PEER-REVIEWED | Posted: 4 October 2023 doi:10.20944/preprints202310.0209.v1

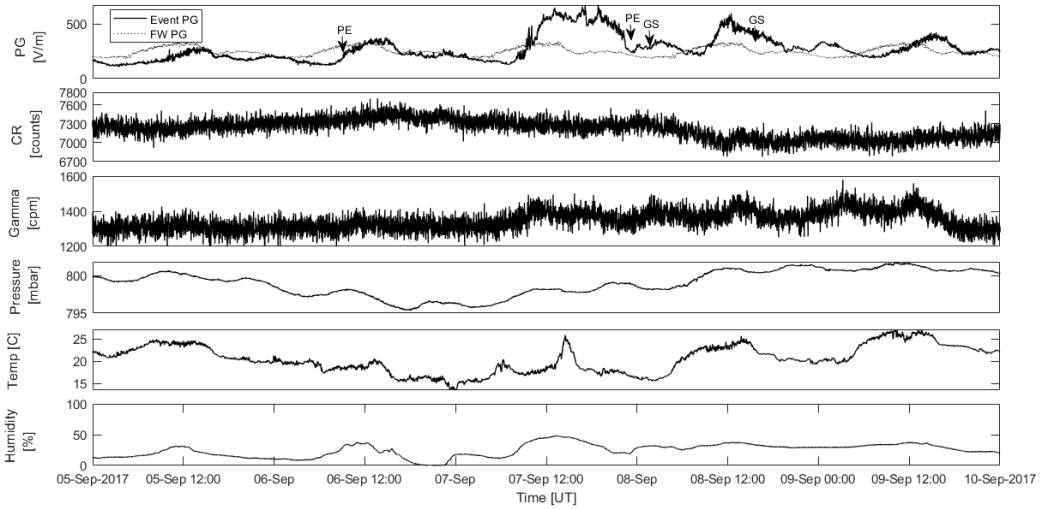

(**b**)

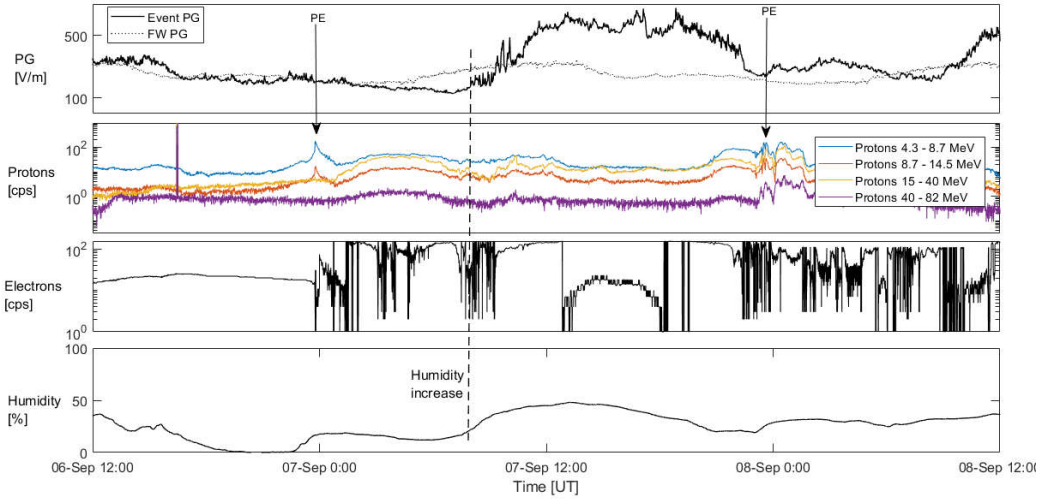

(**c**)

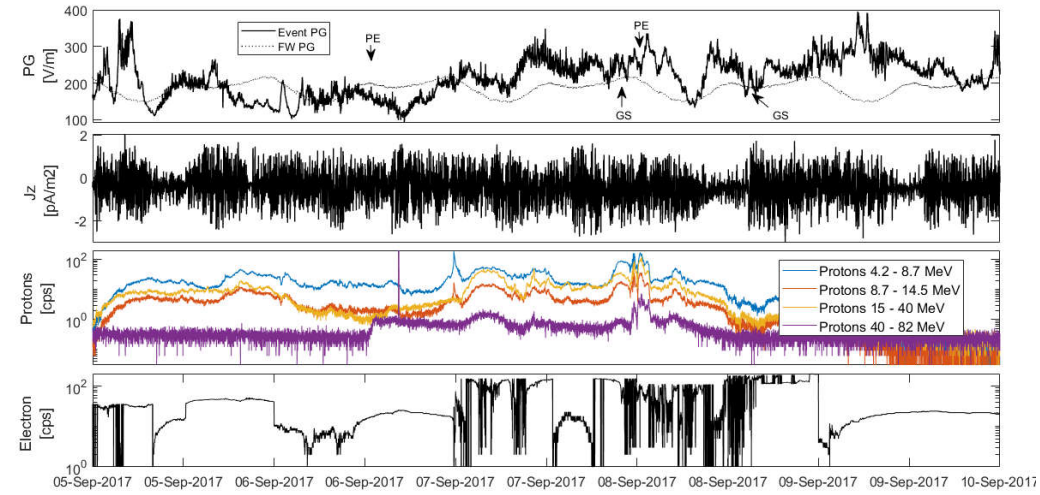

(**d**)

Preprints (www.preprints.org) | NOT PEER-REVIEWED | Posted: 4 October 2023 doi:10.20944/preprints202310.0209.v1

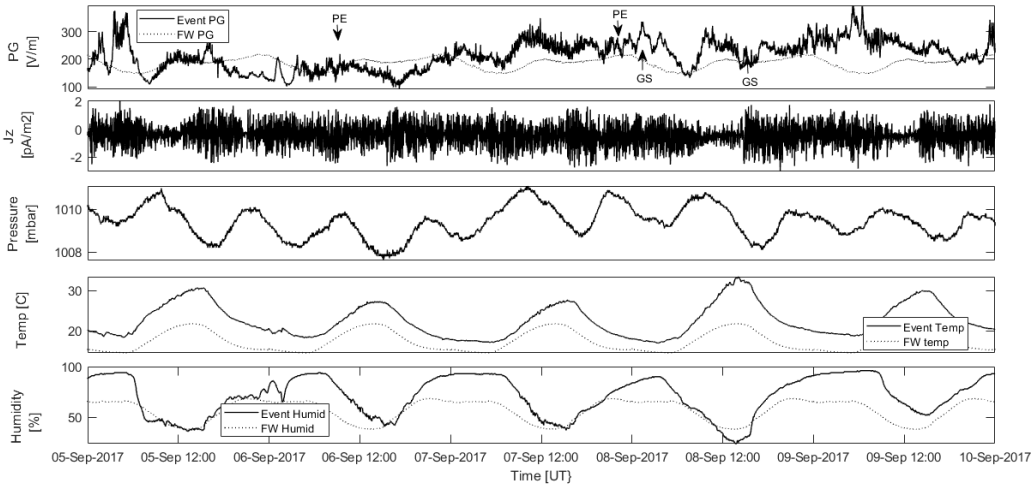

(**e**)

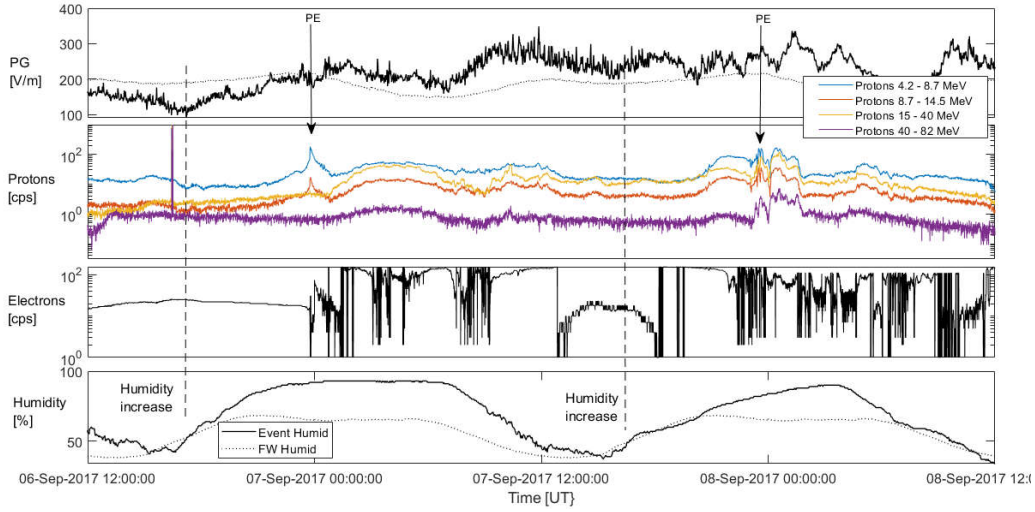

(**f**)

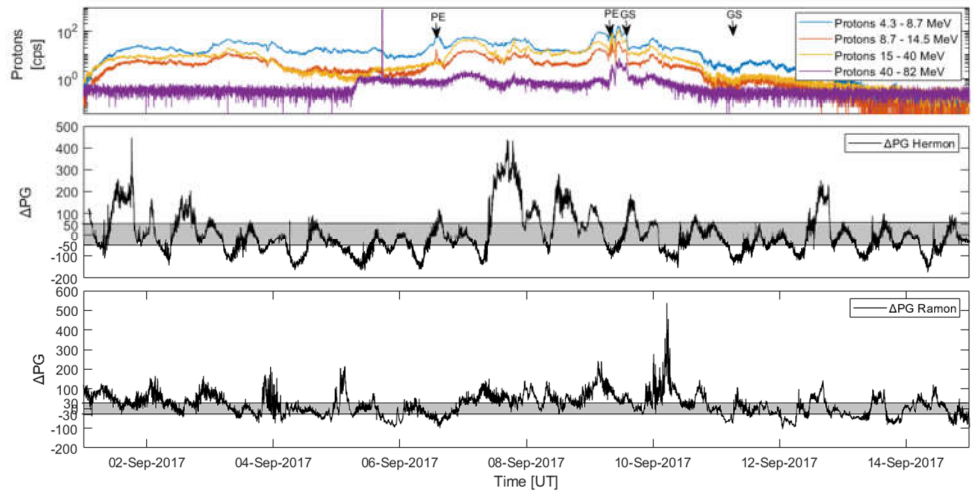

(**g**)

Preprints (www.preprints.org) | NOT PEER-REVIEWED | Posted: 4 October 2023 doi:10.20944/preprints202310.0209.v1

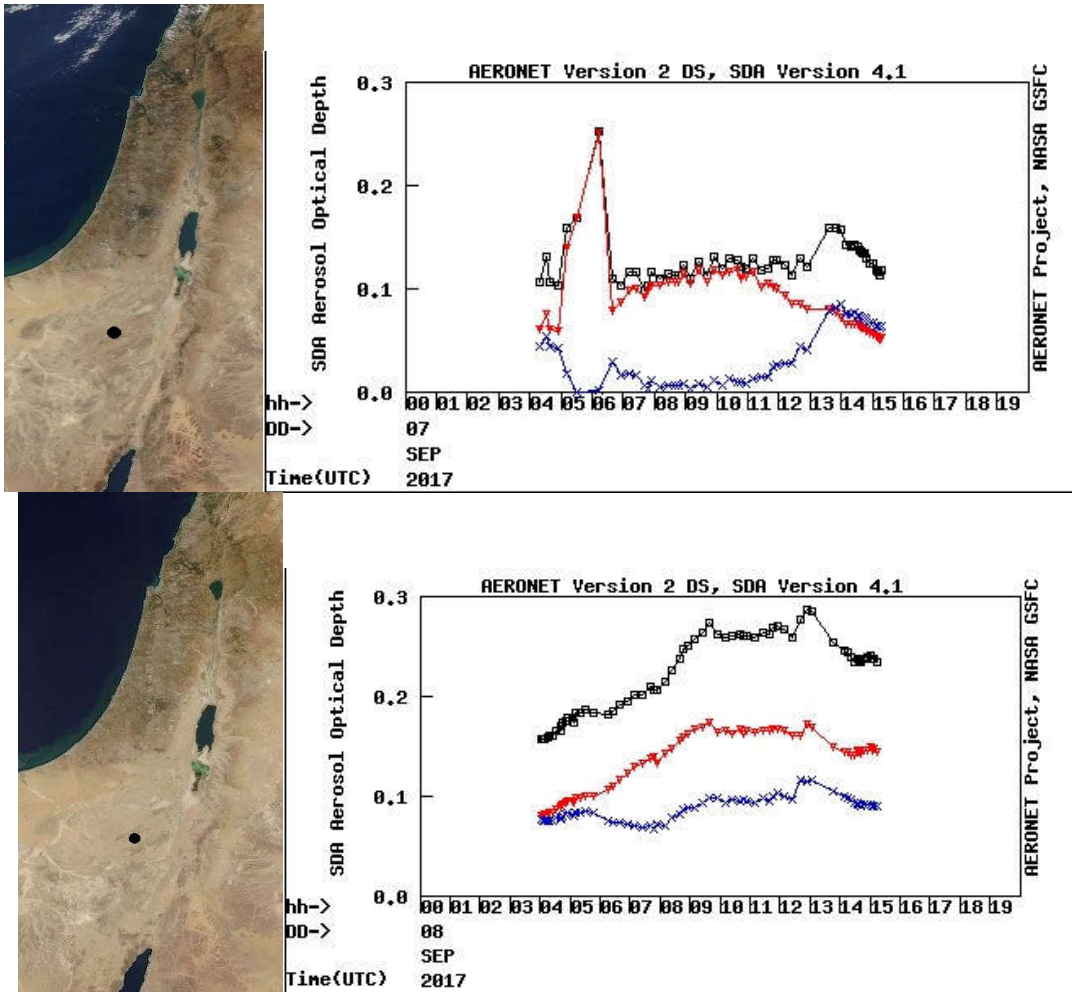

(**h**)

Figure 3. (**a**) 5-10 Sep 2017 Mt. Hermon station parameters: PG (top panel), Cosmic rays intensity counts (Second panel), Gamma detectors (third panel) and the satellite environment measured by GOES 13 - proton and electron flux (bottom panels). (**b**) 5-10 Sep 2017 Mt. Hermon station parameters: PG (top panel), Cosmic rays intensity counts (Second panel), Gamma detectors (third panel) and meteorological parameters of pressure, temperature and humidity (Bottom three panels). Dotted line are mean pattern of fair weather behavior. PE stands for the start of the proton event and GS is the start of the geomagnetic storm. (**c**) Mt. Hermon station zoom-in on the solar event – the parameters are: Protons and electrons flux, PG and Humidity values, dashed line represent the time when humidity starts to increase. (**d**) 5-10 Sep 2017 Mitzpe Ramon station parameters: PG (top panel), Conduction current Jz (Second panel) and meteorological parameters of pressure, temperature and humidity (Bottom three panels). Dotted line show the mean pattern of fair weather behavior. PE stands for the start of the proton event and GS is the start of the geomagnetic storm. (**e**) 5-10 Sep 2017 Mitzpe Ramon station parameters: PG (top panel), Conduction current Jz (Second panel) and the satellite environment measured by GOES 13 - proton and electron flux (bottom panels). (**f**) Mitzpe Ramon station zoom-in on the solar event – the parameters shown are: protons and electrons flux, PG and Humidity values. Dashed line represents the time when humidity starts to increase. (**g**) ΔPG analysis. The solar proton flux with event time indication (top), ΔPG and standard deviation grayed area that show diurnal fair weather variations from the Hermon station (middle) and the Ramon station (bottom). (**h**) Satellite image of Israel showing no clouds at all in the southern region (black dot denotes the MR station) with daily average of fine and coarse particles AOD at from 7 Sep 2017 (top) and 8 Sep 2017 (bottom).

 doi:10.20944/preprints202310.0209.v1

In order to quantify the contributions of meteorological conditions to the electric parameters measured at the ground, one needs to consider the occurrence of clouds, fog, aerosols, high humidity and wind speed parameters, that were found to affect the local Potential Gradient (Yaniv and Yair, 2022; Yair and Yaniv, 2023). For cloudiness data, we used the data archive of the Israeli Meteorological Service (IMS) (https://ims.data.gov.il/ims/1 - The data are open for the public and available in Hebrew and copyrighted to the state of Israel) that provides weather data from Israel including types of clouds, height of cloud base, cloud amounts of low, middle and high clouds in oktas eighths. In addition, we inspected the MODIS infrared and visible Cloud Product data to determine the physical and radiative cloud properties. The data are obtained from the worldview open-source code app website (https://worldview.earthdata.nasa.gov/) and provides interactively browse for global, full-resolution satellite imagery layers with the availability to download the underlying data. The AERONET (AErosol RObotic NETwork) project is an array of ground-based remote sensing aerosol networks established by NASA which provides globally distributed observations of spectral aerosol optical depth (AOD). The station we obtained the data from is located in Sde-Boker, southern Israel (30.855N, 34.782E), approximately 20 km north from the Wise Observatory. Previous studies (Yaniv et al. 2016 and Yair et al. 2016) found that the range of fair-weather mean AOD value at Mitzpe Ramon range from 0.17 – 0.3. Finally, we used local meteorological stations at both sites to obtain weather parameters such as the relative humidity, pressure, temperature and wind speed.

3. Results

Here we present two case studies, which are considered the strongest of the >25 solar events that occurred during the study period (2012-2017). That period coincided with the end of the maximum of solar cycle 24 and the decline period toward solar minimum in 2019-2020. We show the variations of the PG, Jz, CR, gamma ray intensity and the meteorological data, before, during and after the impact of the solar energetic particle (SEP) events on Earth's magnetic field, in search for anomalies that can be attributed to electrical changes in the GEC. In addition, we zoom-in on the period of the day of the event to detect in more detail possible changes in the above-mentioned parameters and plot the difference (ΔPG) between fair weather patterns to PG values measured during a geomagnetic storm induced by a solar event. The start of each event (SEP or geomagnetic storms) caused by a solar event are marked on the graphs by black arrows and designations for “PE” and “GS” for the proton event and geomagnetic storms, respectively. All the times referred to in the figures are UT. Finally, we will try to investigate the contributions, if any was present during the case studies, of other factors (e.g clouds, fog, aerosols) to rule out or understand the combined effects on the PG.

3.1. St. Patrick's Day CME Event 16-20 March 2015

The St. Patrick's Day solar storm had a maximum Kp index = 9, making it the strongest event of 2015. The storm produced a solar proton event from March 16th followed by a strong CME event that arrived at Earth on the morning of March 17th and lasted for more than 24 hours, causing strong disturbances that were measured by the GOES13 satellite (Figure 2a). The variations in the proton flux were followed by strong variations in the electron flux which reached peak values on the midday of March 17th 2015 when the estimated Kp index reached level 9. Figure 2b shows ground measurement of PG, Jz and meteorological data from Mitzpe Ramon (unfortunately, due to technical problems the Mt. Hermon station was out of order during this event). A slight increase of the PG above mean fair weather values was observed during the midnight hours of March 16th increasing to 430 V m^{-1} before reverting back to fair weather values. Throughout this event the conduction current values fluctuated between 1-3 pA m^{-2}. A period with large variation of the conduction current exhibiting values of ~ 400 pA m^{-2} was recorded on March 18th between 12 -18 UT. The episode was accompanied by an increase of the potential gradient. The values of temperature, relative humidity and wind speed were higher than the typical pattern of mean fair-weather behavior (e.g the wind speed was up to 50 km h^{-1} which is much higher than the limit of <30 km h^{-1} of the fair weather criteria (Harrison et al., 2018)). The PG and Jz disturbances occurred during the same period of time of high

relative humidity and strong wind, indicating that the source of fluctuation may be related to local weather patterns, which obscured the solar signal, if it existed at all. On the other hand, the relative humidity and high wind speed values do not imply conditions to generate fog, thus we can negate the PG increase due to the fog factor (Yair and Yaniv, 2023). Figure 2c is a zoom-in of the event and shows that there is slight increase in the PG when the proton flux increase, but the high values and the response above fair-weather values begins several hours after the start of the event and are not immediate (or at least 70 sec delay) as would have been expected compared to past results (Sheftel et al., 1994). The dashed line shows that the increase of the PG is also at the same time when there was an increase in the humidity, as reported recently by Yair and Yaniv (2023). The PG values return to slightly above fair-weather values when the humidity decreased and they rise again when there is a renewal increase of humidity, as expected from the weather-controlled daily cycle (Yaniv et al., 2017). The ΔPG analysis (Figure 2d) reveals a difference of +30-200 V m^{-1} above fair-weather values several hours after the proton event, a fact that supports the idea of PG response due to local meteorological effects. No clouds were observed in satellite images (Figure 2e) above the Mitzpe Ramon station at the time of the solar event, negating the factor of PG variability due to clouds. Aerosol concentration analysis (AOD) at the region during the solar events found values of 0.05 – 0.25 which correspond to fair weather values (Yaniv et al. 2016 and Yair et al. 2016), negating the potential contribution of high aerosol concentrations (Katz et al., 2019).

3.2. CME Event 6-8 September 2017

This solar event was the strongest event of 2017 and the 12th strongest event to date to be recorded by NASA. Figure 3a shows 5 days of space weather data from 5-10 September 2017 and the strong CME which erupted from the sun on September 6th 2017 reaching Earth on the 8th with high fluxes of protons and electrons. The Kp values were above 6, reaching maximum value of Kp=9 throughout September 8th. The 10 MeV proton flux was high (50-100 cps) during the entire period and the high energy protons flux (up to 10 cps) of 50 and 100 MeV were measured on September 6th 2017 at 12UT. Both our stations recorded continuous PG data and we review it below and compare it with space weather parameters.

Figure 3a and 3b presents the PG variations from the Mt. Hermon station (bold black) and the fair-weather PG behavior (black dotted line). The PG values show a clear increase of 150-250 V m^{-1} around September 7th 12 UT. Sadly, the Mt. Hermon Jz station suffered from internal noise and the data was not retrievable. The second panel of figure 3a shows CR counts from Mt. Hermon and exhibit a continuing decrease over a period of several hours of ~400 counts which constitute ~5% of the counts before the event, suggesting a minor Forbush decrease. We should note that cosmic ray data from Mt. Hermon station exhibits a regular daily variation of 0.5% - 1% when space weather conditions are quiet (Dorman 2003), therefore, 5% decrease clearly suggests a Forbush decrease from a solar event.

The gamma detector on Mt. Hermon (third panel in figure 3a) showed an increase of 10-15% (150-200 cpm higher) starting from September 7th and throughout the following day. The bottom three panels in Figure 3b show the meteorological data on the mountain, exhibiting values slightly above the average fair weather values (30% humidity; Harrison et al., 2018). It should be noted that no wind data was available during the event. Figure 3c is a zoom-in on the event which shows that the increase in the PG correlates with the time of increase in the relative humidity suggesting higher concentration of water vapor and a decrease in conductivity followed by an increase in the PG, as measured by Bennet and Harrison (2007). We can rule out the possibility that the change is related to the incoming particle flux, since there was apparent response of the PG to the humidity increase several hours after the event (marked as PE on figure 3b) on the 6th or to the electron flux (marked as GS on figure 3b) on September 8th. The diurnal pattern of the PG at the Hermon station with the "Austausch" effect continued as usual despite this strong space weather event (Yaniv et al., 2017).

Figure 3d and 3e presents the PG variations for the same period of time detected at the Wise Observatory station (bold black) as well as the average fair weather PG behavior (black dotted line). The Mitzpe-Ramon station shows an increase of ~50-150 V m^{-1} compared with fair-weather values.

 doi:10.20944/preprints202310.0209.v1

The Jz data showed no significant departures from fair weather values (Yaniv et al., 2019) and fluctuated between ~±2 pA m^{-2}. The relative humidity showed values above the average, up to 90-100%, that persisted from local evening until noon hours. Such a high humidity indicates fog conditions (Yair and Yaniv 2023). We observe no conspicuous response of the PG to the increase of the low energy proton flux (marked as PE on figure 3a) on September 6th. Similar to the Mt. Hermon results, Figure 3f shows a zoom-in on the event which shows that the values of PG are higher (50 – 250 V m^{-1}) from the fair-weather values during and after the event compared to the days before the event. The ΔPG analysis (Figure 2d) exhibits a difference of +50-250 V m^{-1} and +30-150 V m^{-1} above fair-weather values several hours after the proton event, at both Mt. Hermon and Ramon stations (respectively), suggesting that again, the source of the delayed PG response is a superposition of local meteorological effects, especially high humidity.

No clouds were observed by satellite images from 7 Sep and 8 Sep 2017 (Figure 3h top and bottom) above the Mitzpe Ramon in the time of the solar event, negating the factor of PG increase due to low clouds. Aerosols analysis (AOD) at the region during the solar events found AOD values below 0.3 which are fair weather values according to previous studies (Yaniv et al. 2016 and Yair et al. 2016), negating any PG increase that might result from high aerosol concentration factor.

4. Summary

Two case studies of unusually strong solar proton events accompanied by geomagnetic storms impacting Earth's atmosphere were analyzed, in search for a response of parameters of the Global Electric Circuit at 2 low-latitude stations in Israel. The 2015 St. Patrick day event (case study 1) was an SEP followed by a strong geomagnetic storm of Kp=9, and the September 6-8th 2017 had also reached a maximum Kp=9.

Our analysis ruled out the possibility that the observed PG increase was due to presence of clouds, and high concentrations of aerosols. Still, it is likely that the observed increase of the potential gradient and current density during both case studies can be explained by local temporal meteorological conditions, probably high humidity and strong winds and even fog. The high relative humidity can lead to the formation of small droplets and hydrated ion clusters which reduces atmospheric conductivity (Harrison 2005, Bennet and Harrison 2007, Yair and Yaniv 2023). The strong wind that was measured (~30-50 km h^{-1}) can transport space charge thus affecting the local resistivity, the ambient electric field and current density (Elhalel et al., 2014, Yaniv et al., 2016, Lucas et al., 2017, Yair and Yaniv 2023). Both meteorological effects lower the conductivity and increase the PG, as required by Ohm's law.

The results from the Israeli stations do not agree with past observations (Kleimenova et al 2009, Smirnov 2014, Nicoll and Harrison 2014) that showed an increase of the surface electric field during and after SEP events and geomagnetic storms. We should note an important difference between these observations, stemming from the fact that the majority of past results were obtained at higher latitudes >45N which naturally have lower cut-off rigidity values (~3 GV and lower) where the magnetospheric shielding is less intense, compared to the 10.3 GV at the latitudes of Israel, ~30N (Makhmutov et al., 2015). Similar low latitude station in Argentina (9.8 GV cutoff rigidity) show that the impact on PG was found to be of the order of ~10-15 V m^{-1} (Tacza et al. 2018) an almost negligible offset that can be easily masked by local meteorological conditions. Based on the known variations of the fair-weather potential gradient of ±30 V m^{-1} and ±50 V m^{-1} at Mitzpe Ramon and Mt. Hermon, respectively (Yaniv et al., 2016, 2017), our results suggest that ionization effects and PG changes due to strong solar events were entirely masked and were below detection threshold, and thus cannot be observed in the geographical latitudes of Israel. A possible interpretation of the results suggests that even the strongest solar events, that generate geomagnetic storms with electron fluxes (~1 MeV) and solar energetic particle events (proton fluxes higher than 10 Mev), are effectively shielded at low latitudes (30°N), such as the locations of our two stations in Israel. This shielding precludes the appearance of significant signals in the ambient electric field at surface level that may be conspicuous above the normal fair weather fluctuations, which are always dominated by local daily meteorological factors, such as high humidity and wind.

Acknowledgments: This research was supported by the Israel Science Foundation (grant No. 423/14). Sunspot Numbers data - SILSO data/image, Royal Observatory of Belgium, Brussels. GOES data - http://www.swpc.noaa.gov.

References

1. Bennett, A. J., & Harrison, R. G. (2007). Atmospheric electricity in different weather conditions. *Weather*, *62*(10), 277-283.
2. Bennett, A. J., & Harrison, R. G. (2008). Surface measurement system for the atmospheric electrical vertical conduction current density, with displacement current density correction. *Journal of atmospheric and solar-terrestrial physics*, *70*(11-12), 1373-1381.
3. Cobb, W. E. (1967). Evidence of a solar influence on the atmospheric electric elements at Mauna Loa Observatory. *Mon. Weather Rev*, *95*(12), 905-911.
4. Elhalel, G., Yair, Y., Nicoll, K., Price, C., Reuveni, Y., & Harrison, R. G. (2014). Influence of short-term solar disturbances on the fair weather conduction current. *Journal of Space Weather and Space Climate*, *4*, A26.
5. Dorman, L. (2013). *Cosmic rays in the Earth's atmosphere and underground* (Vol. 303). Springer Science & Business Media.
6. Gurevich, A. V., Zybin, K. P., & Roussel-Dupre, R. A. (1999). Lightning initiation by simultaneous effect of runaway breakdown and cosmic ray showers. *Physics Letters A*, *254*(1-2), 79-87.
7. Gurevich, A. V., & Zybin, K. P. (2005). Runaway breakdown and the mysteries of lightning. *Phys. Today*, *58*(5), 37-43.
8. Harrison, R. G. (2005). Columnar resistance changes in urban air. *Journal of atmospheric and solar-terrestrial physics*, *67*(8-9), 763-773.
9. Harrison, R. G. (2013). The carnegie curve. *Surveys in Geophysics*, *34*(2), 209-232.
10. Harrison, R. G., & Nicoll, K. A. (2018). Fair weather criteria for atmospheric electricity measurements. *Journal of Atmospheric and Solar-Terrestrial Physics*, *179*, 239-250.
11. Haldoupis, C., Rycroft, M., Williams, E., & Price, C. (2017). Is the "Earth-ionosphere capacitor" a valid component in the atmospheric global electric circuit?. *Journal of Atmospheric and Solar-Terrestrial Physics*, *164*, 127-131.
12. Holzworth, R. H. (1981). High latitude stratospheric electrical measurements in fair and foul weather under various solar conditions. *Journal of Atmospheric and Terrestrial Physics*, *43*(11), 1115-1125.
13. Holzworth, R. H., Norville, K. W., & Williamson, P. R. (1987). Solar flare perturbations in stratospheric current systems. *Geophysical research letters*, *14*(8), 852-855.
14. -Hudson, H. S. (2011). Global properties of solar flares. *Space Science Reviews*, *158*(1), 5-41.
15. Kallenrode, M. B. (2003). An Introduction to Plasmas and Particles in the Heliosphere and Magnetospheres.
16. Kasatkina, E. A., Shumilov, O. I., Rycroft, M. J., Marcz, F., & Frank-Kamenetsky, A. V. (2009). Atmospheric electric field anomalies associated with solar flare/coronal mass ejection events and solar energetic charged particle" Ground Level Events". *Atmospheric Chemistry and Physics Discussions*, *9*(5), 21941-21958.
17. Kleimenova, N., Kozyreva, O., Kubicki, M., & Michnowski, S. (2009). Variations of the mid-latitude atmospheric electric field (Ez) associated with geomagnetic disturbances and Forbush decreases of cosmic rays. *Recent developments in Atmospheric Electricity, Publs. Inst. Geophys. Pol. Acad. Sci. D-73*, *412*, 55-64.
18. Lucas, G. M., Thayer, J. P., & Deierling, W. (2017). Statistical analysis of spatial and temporal variations in atmospheric electric fields from a regional array of field mills. *Journal of Geophysical Research: Atmospheres*, *122*(2), 1158-1174.
19. Makhmutov, V., Bazilevskaya, G., Stozhkov, Y., Philippov, M., Yair, Y., Yaniv, R., Harrison G., Nicoll K. and Aplin, K., (2015). Cosmic ray measurements in the atmosphere at several latitudes in October 2014. *PoS*, 392.
20. Mezuman, K., Price, C., & Galanti, E. (2014). On the spatial and temporal distribution of global thunderstorm cells. *Environmental Research Letters*, *9*(12), 124023.
21. Mironova, I. A., Aplin, K. L., Arnold, F., Bazilevskaya, G. A., Harrison, R. G., Krivolutsky, A. A., ... & Usoskin, I. G. (2015). Energetic particle influence on the Earth's atmosphere. *Space Science Reviews*, *194*(1-4), 1-96.
22. Miyahara, H., Higuchi, C., Terasawa, T., Kataoka, R., Sato, M., & Takahashi, Y. (2017). Solar 27-day rotational period detected in wide-area lightning activity in Japan. In *Annales Geophysicae* (Vol. 35, No. 3, p. 583). Copernicus GmbH.

23. Neto, O. P., Pinto, I. R., & Pinto Jr, O. (2013). The relationship between thunderstorm and solar activity for Brazil from 1951 to 2009. *Journal of Atmospheric and Solar-Terrestrial Physics*, *98*, 12-21.
24. Nicoll, K. A., & Harrison, R. G. (2014). Detection of lower tropospheric responses to solar energetic particles at midlatitudes. *Physical review letters*, *112*(22), 225001.
25. Nikiforova, N. N., Kleimenova, N. G., Kozyreva, O. V., Kubitski, M., & Michnowski, S. (2005). Unusual variations in the atmospheric electric field during the main phase of the strong magnetic storm of October 30, 2003, at Swider Polish midlatitude observatory. *Geomagnetism and Aeronomy*, *45*(1), 140-144.
26. Qiu, S., Xie, Y., Shi, M., Yousof, H., Soon, W., Ren, Z., ... & Dou, X. Observations and analysis of the mid-latitude atmospheric electric field during geomagnetic activity. Journal of Geophysical Research: Space Physics, e2022JA030785.
27. Reiter, R. (1969). Solar flares and their impact on potential gradient and air-earth current characteristics at high mountain stations. *pure and applied geophysics*, *72*(1), 259-267.
28. Reuveni, Y., & Price, C. (2009). A new approach for monitoring the 27-day solar rotation using VLF radio signals on the Earth's surface. *Journal of Geophysical Research: Space Physics*, *114*(A10).
29. Reuveni, Y., Yair, Y., Price, C., & Steinitz, G. (2017). Ground level gamma-ray and electric field enhancements during disturbed weather: Combined signatures from convective clouds, lightning and rain. *Atmospheric Research*, *196*, 142-150.
30. Roussel-Dupré, R., Colman, J. J., Symbalisty, E., Sentman, D., & Pasko, V. P. (2008). Physical processes related to discharges in planetary atmospheres. In *Planetary Atmospheric Electricity* (pp. 51-82). Springer, New York, NY.
31. Rycroft, M. J., Israelsson, S., & Price, C. (2000). The global atmospheric electric circuit, solar activity and climate change. *Journal of Atmospheric and Solar-Terrestrial Physics*, *62*(17-18), 1563-1576.
32. Rycroft, M. J., Nicoll, K. A., Aplin, K. L., & Harrison, R. G. (2012). Recent advances in global electric circuit coupling between the space environment and the troposphere. *Journal of Atmospheric and Solar-Terrestrial Physics*, *90*, 198-211.
33. Scott, C. J., Harrison, R. G., Owens, M. J., Lockwood, M., & Barnard, L. (2014). Evidence for solar wind modulation of lightning. *Environmental Research Letters*, *9*(5), 055004.
34. Sheftel, V. M., Bandilet, O. I., Yaroshenko, A. N., & Chernyshev, A. K. (1994). Space-time structure and reasons of global, regional, and local variations of atmospheric electricity. *Journal of Geophysical Research: Atmospheres*, *99*(D5), 10797-10806.
35. Smirnov, S. (2014). Reaction of electric and meteorological states of the near-ground atmosphere during a geomagnetic storm on 5 April 2010. *Earth, Planets and Space*, *66*(1), 1-8.
36. Tacza, J., Raulin, J. P., Macotela, E., Norabuena, E., Fernandez, G., Correia, E., ... & Harrison, R. G. (2014). A new South American network to study the atmospheric electric field and its variations related to geophysical phenomena. *Journal of Atmospheric and Solar-Terrestrial Physics*, *120*, 70-79.
37. Tacza, J., Raulin, J. P., Mendonca, R. R. S., Makhmutov, V. S., Marun, A., & Fernandez, G. (2018). Solar effects on the atmospheric electric field during 2010–2015 at low latitudes. *Journal of Geophysical Research: Atmospheres*, *123*(21), 11-970.
38. Tinsley, B. A. (1996). Correlations of atmospheric dynamics with solar wind-induced changes of air-Earth current density into cloud tops. *Journal of Geophysical Research: Atmospheres*, *101*(D23), 29701-29714.
39. Yaniv, R., Yair, Y., Price, C., & Katz, S. (2016). Local and global impacts on the fair-weather electric field in Israel. *Atmospheric research*, *172*, 119-125.
40. Yaniv, R., Yair, Y., Price, C., Mkrtchyan, H., Lynn, B., & Reymers, A. (2017). Ground-based measurements of the vertical E-field in mountainous regions and the "Austausch" effect. *Atmospheric research*, *189*, 127-133.
41. Yaniv, R., Reuveni, Y., Yair, Y., & Lynn, B. (2019). Temporal variations of the conduction current density during fair weather days in Israel. *Atmospheric research*, *222*, 1-11.
42. Yaniv, R., and Yair, Y. (2022). Electric Field Variations Caused by Low, Middle and High-Altitude Clouds over the Negev Desert, Israel. Atmosphere, 13(8), 1331.
43. Yair, Y., & Yaniv, R. (2023). The effects of fog on the atmospheric electrical field close to the surface. Atmosphere, 14(3), 549.

44. Whipple, F. J. W. (1929). On the association of the diurnal variation of electric potential gradient in fine weather with the distribution of thunderstorms over the globe. *Quarterly Journal of the Royal Meteorological Society*, *55*(229), 1-18.
45. Zhao, L. L., & Zhang, H. (2016). Transient galactic cosmic-ray modulation during solar cycle 24: A comparative study of two prominent Forbush decrease events. *The Astrophysical Journal*, *827*(1), 13.